DARPP32, a target of hyperactive mTORC1 in the retinal pigment epithelium

Jiyang Cai[a] , Christopher Litwin[b,c], Rui Cheng[d], Jian-Xing Ma[d], and Yan Chen[b,c,e,1]

The mechanistic target of rapamycin (mTOR) is assembled into signaling complexes of mTORC1 or mTORC2, and plays key roles in cell metabolism, stress response, and nutrient and growth factor sensing. Accumulating evidence from human and animal model studies has demonstrated a pathogenic role of hyperactive mTORC1 in age-related macular degeneration (AMD). The retinal pigment epithelium (RPE) is a primary injury site in AMD. In mouse models of RPE-specific deletion of Tuberous sclerosis 1 (_Tsc1_), which encodes an upstream suppressor of mTORC1, the hyperactivated mTORC1 metabolically reprogrammed the RPE and led to the degeneration of the outer retina and choroid (CH). In the current study, we use single-cell RNA sequencing (scRNA-seq) to identify an RPE mTORC1 downstream protein, dopamine- and cyclic AMP-regulated phosphoprotein of molecular weight 32,000 (DARPP-32). DARPP-32 was not found in healthy RPE but localized to drusen and basal linear deposits in human AMD eyes. In animal models, overexpressing DARPP-32 by adeno-associated virus (AAV) led to abnormal RPE structure and function. The data indicate that DARPP-32 is a previously unidentified signaling protein subjected to mTORC1 regulation and may contribute to RPE degeneration in AMD.

mTORC1 | age-related macular degeneration | RPE | drusen

Hyperactivated mTORC1 is a mechanism of retinal pigment epithelium (RPE) degeneration in age-related macular degeneration (AMD) (1–6). RPE provides essential support to the neural retina (7) and is vital to the choroidal vasculature, especially the choriocapillaris. Mice with an RPE-specific _Tsc1_ knockout (_Tsc1_[RPE_KO]) displayed AMD-like pathology, such as choroidal thinning and loss of vascular area, and outer retina degeneration. The phenotype cannot be attributed to the known functions of mTORC1 downstream proteins (3, 6). The main goal of the current study is to identify candidate proteins that can mechanistically link mTORC1 hyperactivation and RPE degeneration.

Results and Discussion

With bulk RNA sequencing (6), we found that _Darpp-32_ (also known as _Ppp1r1b_) (8, 9) was a top candidate of differentially expressed genes that were significantly up-regulated in the RPE/choroid (CH) tissue of _Tsc1_[RPE_KO] mice (Fig. 1_A_). The selective up-regulation of the _Ppp1r1b_ messenger RNA in the RPE was further confirmed with single-cell RNA sequencing (scRNA-seq) analyses. The single-cell suspension of RPE/CH was prepared (10) and barcoded on the 10× Genomics platform. Data analyses and cell clustering were performed in Seurat (11), and annotated with known cell markers (Fig. 1_B_) (10, 12). There was negligible transcription of _Ppp1r1b_ in the RPE in the control mice. In the _Tsc1_[RPE_KO] mice, increased _Ppp1r1b_ transcripts were identified mainly in the cluster of cells expressing RPE-specific markers _Rpe65_ and _Rdh5_ (Fig. 1 _B–D_).

To confirm the scRNA-seq findings on the protein level, we performed immunostaining on both posterior eye cryosections and flat-mounted RPE/CH tissue. In _Tsc1_-floxed mice, DARPP-32 was mainly expressed in the inner retina, with minimal staining in the RPE (Fig. 1_E_) (13). In _Tsc1_[RPE_KO] mice, in addition to the retina, the RPE showed robust DARPP-32 staining. On RPE flat mounts, there was minimal punctate staining of DARPP-32 in the flox mice, supporting low RPE expression of DARPP-32 under normal conditions (Fig. 1_F_). In _Tsc1_[RPE_KO] mice, DARPP-32 positive signals were readily detected in RPE cells, although the fluorescence intensity of the staining varied among individual cells (Fig. 1_F_). On Western blots (Fig. 1_G_), the level of DARPP-32 was significantly increased in TSC1-deficient RPE compared to the flox littermates (Fig. 1 _G_ and _H_). Knockout of _Tsc1_ led to increased S6 phosphorylation (Fig. 1_G_), confirming the high mTORC1 activity. These data collectively support
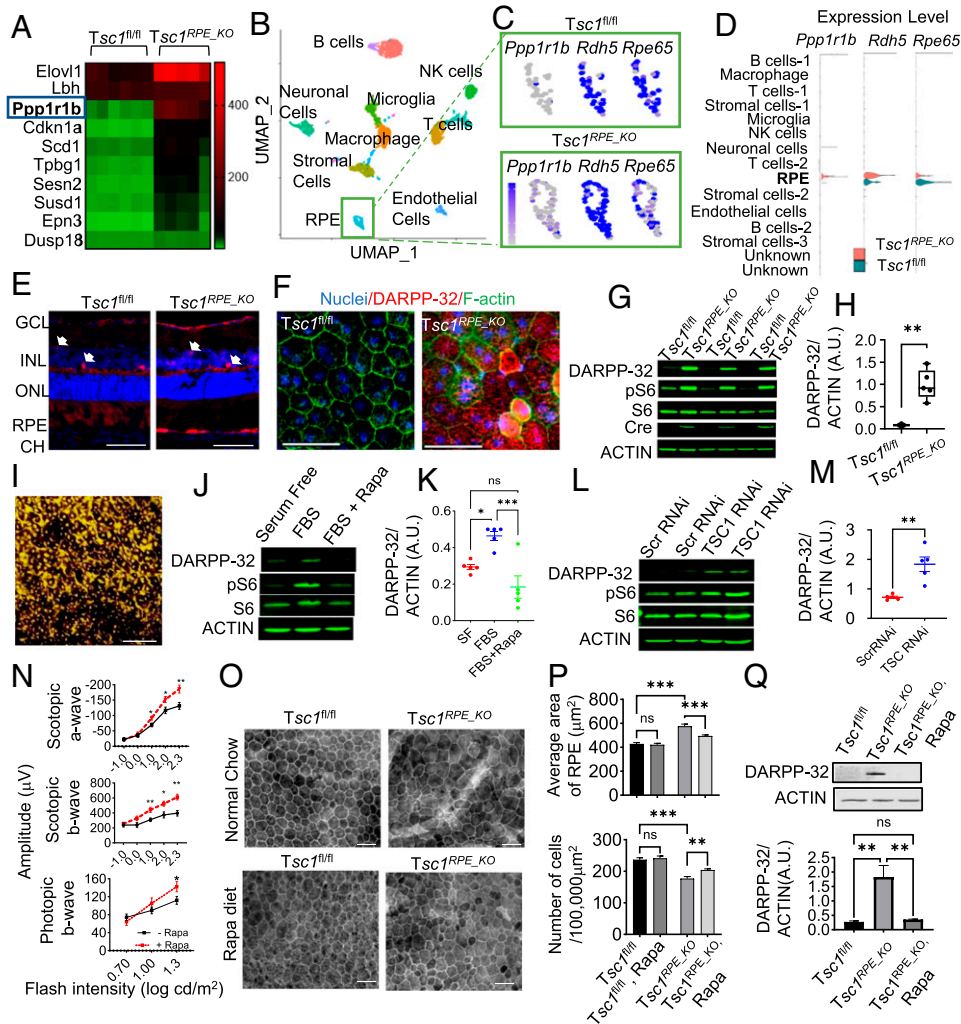
Fig. 1. Up-regulation of DARPP-32 in the RPE with hyperactive mTORC1. (*A*) Heatmap plot of the top 10 genes differentially expressed in the *Tsc1*-deficient RPE/CH transcriptome. (*B–D*) The scRNA-seq analysis on RPE/CH tissues. (*B*) Uniform Manifold Approximation and Projection (UMAP) plot of single-cell clusters of RPE/CH. Cells prepared from *Tsc1*^RPE_KO and *Tsc1*-floxed mice were integrated for the analysis. (*C* and *D*) Increased *Ppp1r1b* in the RPE cluster of *Tsc1*^RPE_KO mice. (*E* and *F*) Immunostaining of posterior eye cryosections and RPE/CH flat mounts. The results are the representation of three animals. Arrows indiate positive staining of DARPP-32 (*G* and *H*) Western blot analysis and quantification of total DARPP-32 expression in the RPE-enriched fraction, normalized to β-actin; n = 5; ~2- to ~3-mo-old mice were used. (*I*) A representative brightfield image of cultured primary mRPE cells. (*J* and *K*) Representative images and quantification of Western blot of mRPE cells stimulated with FBS for 4 h, in the presence or absence of rapamycin (Rapa). (*L* and *M*) Representative image and quantification of Western blot of human ARPE-19 cells transfected with small interference RNA against *Tsc1* or the scramble control. The results are from five separate experiments. (*N*) ERG measurement in *Tsc1*^RPE_KO mice, on control or Rapa-supplemented diet for 5 mo. Experiments were started in mice at ~2 mo to ~3 mo of age (n = 6). (*O*) F-actin staining of RPE flat mounts. (*P*) The average size and number of RPE cells in the middle periphery region are quantified and presented; 3 or 4 animals per group. (*Q*) Representative Western blots and quantification of DARPP-32 expression in the RPE of animals on Rapa supplement or control chow. The expression of DARPP-32 was normalized to the expression of actin. (n = 4). *$P < 0.05$, **$P < 0.01$, ***$P < 0.001$, ns $P \geq 0.05$. (Scale bars: 50 μm).

an abnormal accumulation of DARPP-32 transcript and protein in the RPE with hyperactive mTORC1.

To establish the causative link between mTORC1 activation and up-regulation of DARPP-32, we used cultured primary mouse RPE cells (mRPE) at confluency (Fig. 1*I*) to test whether DARPP-32 can be induced by fetal bovine serum (FBS). FBS activated mTORC1 in primary mRPE as measured by the S6 phosphorylation. The same treatment led to increased DARPP-32 (Fig. 1*J*). The prototypical mTORC1 inhibitor, rapamycin, substantially inhibited S6 phosphorylation and lowered DARPP-32 to below the control level, supporting that DARPP-32 is a downstream target of mTORC1 activation in the RPE (Fig. 1 *J* and *K*). Similar to the in vivo findings from *Tsc1*^RPE_KO mice, depletion of TSC1 by RNA interference in the immortalized human ARPE-19 cells led to activation of mTORC1 and increased expression of DARPP-32 (Fig. 1 *L* and *M*). We further examined whether mTORC1 inhibition in vivo can impact the level of DARPP-32 in the RPE. The *Tsc1*^RPE_KO mice were kept on either a rapamycin-supplemented diet (containing 14 ppm active rapamycin) or a control diet for 5 mo. Similar to a previous report (3), rapamycin improved the scotopic and photopic electroretinogram (ERG) responses (Fig. 1*N*) and RPE morphology (Fig. 1 *O* and *P*) in *Tsc1*^RPE_KO mice. When RPE/choroid tissues were analyzed by Western blot, the amount of DARPP-32 in *Tsc1*^RPE_KO mice was reduced by rapamycin to a level comparable to that in control flox mice (Fig. 1*Q*). Altogether, the results from in vitro and in vivo studies further support that

DARPP-32 accumulation was a downstream event of hyperactive mTORC1 signaling in the RPE.

To examine the functional outcome of DARPP-32 overexpression in the RPE, we performed subretinal injection of adeno-associated virus 2 (AAV2) encoding mouse DARPP-32. The overexpression of the protein in the RPE was confirmed on RPE whole mounts (Fig. 2*A*). We examined RPE morphology on flat-mounted RPE tissues 5 mo after injection. Control AAV vector did not cause an apparent morphological change of the RPE, while overexpression of DARPP-32 caused RPE degenerative changes as indicated by the loss of hexagonal/pentagonal morphology and abnormally large or small size (Fig. 2*B*). In addition, the RPE had increased expression of α-SMA, a fibrosis marker, suggesting degeneration/dedifferentiation of the RPE (Fig. 2*C*). When the AAV-injected mice were subjected to ERG measurement (Fig. 2*D*), the c-wave amplitude was reduced after DARPP32 overexpression, indicating impaired RPE function.

To establish the association of increased expression of DARPP-32 in the RPE with the pathogenesis of AMD, we stained paraffin sections of posterior eyes from human AMD patients and age-matched control subjects. In control subjects, DARPP-32 was detected in the inner retina (14) and occasionally in drusen (Fig. 2*H*). In AMD eyes, DARPP-32 showed positive staining in macular and peripheral drusen (Fig. 2 *J* and *L*), RPE basal linear deposits (Fig. 2*L*), and degenerating RPE cells (Fig. 2*N*). The intensity of the signals under the RPE was much stronger than that in the retina. The number of DARPP32-positive structures
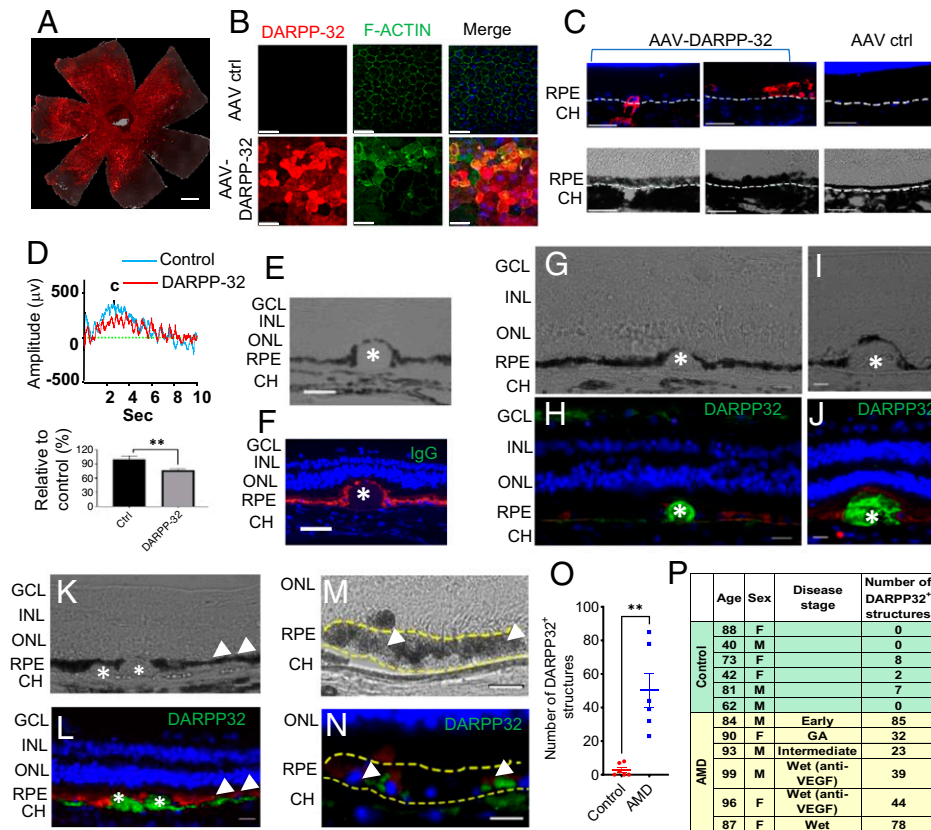
Fig. 2. Overexpression of DARPP-32 in the RPE led to degeneration. (*A*) A representative image of DARPP-32 immunostaining (red) on RPE whole mount after AAV-delivered overexpression of mouse DARPP-32; *n* = 2. (*B*) F-actin and DARPP-32 staining of RPE/choroid flat mount after AAV delivery; *n* = 3. (*C*) Immunostaining of α-SMA in the RPE with DARPP-32 overexpression or control AAV (ctrl). Five of the five biological replicates examined had positive staining areas in the RPE. (*D*) ERG c wave in mice injected with AAV-DARPP-32 or ctrl; *n* = 8. (*E–N*) Immunostaining of human posterior eye globes paraffin sections: (*G* and *H*) from a control subject (73 y old, F); (*E, F,* and *I–N*) from AMD subjects; (*E, F,* and *I*) from one patient, 96 y old, wet AMD and anti-VEGF injection; (*J*) from one patient, 84 y old, early-stage AMD; and (*M* and *N*) from one patient, 87 y old, wet AMD. Green, DARPP-32 or control IgG; red, RPE autofluorescence; blue, DAPI; asterisk, drusen; arrows, basal liner deposits/degenerating RPE. The dashed lines indicate the apical and the basal side of the RPE. (*O*) Comparisons between control and AMD eyes on DARPP32-positive staining. (*P*) Demographic information of donors. Scale bars: 500 μm in (*A*) and 50 μm in others. **$P < 0.01$.

	Age	Sex	Disease stage	Number of DARPP32+ structures
Control	88	F		0
	40	M		0
	73	F		8
	42	M		2
	81	M		7
	62	M		0
AMD	84	M	Early	85
	90	F	GA	32
	93	M	Intermediate	23
	99	M	Wet (anti-VEGF)	39
	96	F	Wet (anti-VEGF)	44
	87	F	Wet	78

was markedly increased in eyes with AMD (Fig. 2*O*), supporting a contributing role of the protein to the pathogenesis of AMD.

Currently, there is no effective cure for the dry form of AMD, a condition that accounts for over 85% of AMD patients and leads to progressive vision loss. We and others have shown that overactivation of the mTORC1 in the RPE is a major pathogenic mechanism of dry AMD. However, clinical trials using rapamycin were unsuccessful (15). In contrast to the RPE, retinal neurons rely on mTORC1 for their proper functions. Inhibiting mTORC1, especially in eyes with existing geographic atrophy, can cause retinal toxicity despite the benefits of rapamycin in the RPE. Therefore, there is an unmet need to identify new interventional strategies that are based on mTORC1 downstream proteins with unique functions in diseased RPE and dry AMD. Our current studies identified a downstream protein of mTORC1, DARPP-32, that had low expression in healthy RPE and was robustly up-regulated in the degenerating tissue. The presence of the protein in drusen and degenerating RPE from the human samples indicated the possible pathogenic roles of the protein in AMD and can potentially be a new therapeutic target for dry AMD.

Materials and Methods

Mice and scRNA-seq. *Tsc1*^RPE_KO mice were generated as described previously (6). Viable cells were sorted by flow cytometry from single-cell suspension of RPE/choroid and analyzed by 10× Genomics Chromium (10).

Immunofluorescence Staining of Human Eye Tissues. Human donor eyes were obtained from Lions Gift of Sight and processed for paraffin sections. Anti-DARPP32 antibody staining was performed after antigen retrieval and autofluorescence quenching. Images were taken from both macular and peripheral retina.

All other experiments were performed as described previously (6). Detailed descriptions are provided in *SI Appendix*.

Data, Materials, and Software Availability. All study data are included in the article and/or *SI Appendix*.

1. C. Zhao et al., mTOR-mediated dedifferentiation of the retinal pigment epithelium initiates photoreceptor degeneration in mice. *J. Clin. Invest.* **121**, 369–383 (2011).
2. M. Zhang et al., Dysregulated metabolic pathways in age-related macular degeneration. *Sci. Rep.* **10**, 2464 (2020).
3. J. Huang et al., Abnormal mTORC1 signaling leads to retinal pigment epithelium degeneration. *Theranostics* **9**, 1170–1180 (2019).
4. J. S. Zigler Jr. et al., Mutation in the βA3/A1-crystallin gene impairs phagosome degradation in the retinal pigmented epithelium of the rat. *J. Cell Sci.* **124**, 523–531 (2011).
5. G. Kaur et al., Aberrant early endosome biogenesis mediates complement activation in the retinal pigment epithelium in models of macular degeneration. *Proc. Natl. Acad. Sci. U.S.A.* **115**, 9014–9019 (2018).
6. Y. M. Go et al., MTOR-initiated metabolic switch and degeneration in the retinal pigment epithelium. *FASEB J.* **34**, 12502–12520 (2020).
7. J. B. Hurley, Retina metabolism and metabolism in the pigmented epithelium: A busy intersection. *Annu. Rev. Vis. Sci.* **7**, 665–692 (2021).
8. M. Yger, J. A. Girault, DARPP-32, Jack of all trades … master of which? *Front. Behav. Neurosci.* **5**, 56 (2011).
9. P. Greengard, P. B. Allen, A. C. Nairn, Beyond the dopamine receptor: The DARPP-32/protein phosphatase-1 cascade. *Neuron* **23**, 435–447 (1999).
10. G. L. Lehmann et al., Single-cell profiling reveals an endothelium-mediated immunomodulatory pathway in the eye choroid. *J. Exp. Med.* **217**, e20190730 (2020).
11. A. Butler, P. Hoffman, P. Smibert, E. Papalexi, R. Satija, Integrating single-cell transcriptomic data across different conditions, technologies, and species. *Nat. Biotechnol.* **36**, 411–420 (2018).
12. A. P. Voigt et al., Single-cell transcriptomics of the human retinal pigment epithelium and choroid in health and macular degeneration. *Proc. Natl. Acad. Sci. U.S.A.* **116**, 24100–24107 (2019).
13. P. Witkovsky, P. Svenningsson, L. Yan, H. Bateup, R. Silver, Cellular localization and function of DARPP-32 in the rodent retina. *Eur. J. Neurosci.* **25**, 3233–3242 (2007).
14. B. Meister, U. Arvidsson, H. C. Hemmings Jr., P. Greengard, T. Hökfelt, Dopamine- and adenosine-3′:5′-monophosphate (cAMP)-regulated phosphoprotein of Mr 32,000 (DARPP-32) in the retina of cat, monkey and human. *Neurosci. Lett.* **131**, 66–70 (1991).
15. P. A. Petrou et al., Intravitreal sirolimus for the treatment of geographic atrophy: Results of a phase I/II clinical trial. *Invest. Ophthalmol. Vis. Sci.* **56**, 330–338 (2014).